A Method of Motion Tracking during CT for Motion Correction

Jung-Ha Kim, Johan Nuyts, Zdenka Kuncic and Roger Fulton, *Member, IEEE*

***Abstract*– Patient motion is a significant problem in pediatric PET/CT, and motion correction techniques could potentially remove the need for anaesthesia or sedation that are normally required for very young patients. Effective methods exist for motion correction of neurological PET images, and although there is a scarcity of equivalent methods for CT, a potential method of correcting for rigid head motion during the CT scan has recently been proposed. In this study, we describe a motion tracking method for CT using an optical motion tracking system. Since pose is reported in tracker coordinates, and motion correction requires motion in CT scanner coordinates, a calibration is required to determine the transformation needed to convert between the coordinate systems. We describe such a calibration method, and evaluate it by acquiring two CT scans of a Hoffman 3D brain phantom, with a tracker target attached, in different poses. The applied motion between two scans was calculated from the change in target pose measured by the tracker, and converted to scanner coordinates. This motion was applied to one of the reconstructed image volumes, which was then compared with the other image volume. The mean registration error of the two volumes was estimated from landmark analysis to be less than 0.3 mm on average in all directions, which agreed well with a calculated maximum uncertainty of 0.7 mm. Errors of this magnitude could be acceptable if the CT scans were only used for attenuation correction, but may need to be further reduced for motion correction applications. We anticipate that this will be achievable with improvements to our technique, and intend in future work to use motion data to attempt motion correction in spiral CT studies.**

I. Introduction

PATIENT motion is a significant problem in pediatric PET/CT, particularly in very young patients who routinely require anaesthesia or sedation during scans to prevent motion artifacts [1]. Motion correction techniques could potentially alleviate the need for these interventions. However, although effective methods exist for motion correction of neurological PET images [2, 3], there appears to be no comparable method of correcting for head motion during the CT scan. In order to remove the need for anaesthesia or sedation in PET/CT scans, it is important to be able to perform motion correction during CT as well as PET scans.

CT motion artifacts occur due to violation of the assumption made in the reconstruction algorithm that the object remains stationary while projection data are collected. This assumption is often not true in clinical studies. Patient motion results in data inconsistencies that appear as distortion or blurring of the image [4].

Some previous studies have quantified the amount of patient motion during CT scans and the effect of motion artifacts on diagnosis. Wagner *et al*., reported head movement in all CT scans in a cohort of 20 patients [5], and in a more recent study Plessis *et al*. [6] found approximately 43% of pediatric patients aged 0 to 13 years demonstrated motion artifacts in CT scans. Of these, 20% were misinterpreted, leading to false diagnoses and unnecessary further investigations. In PET/CT scans, motion corrupted CT images can result in significant mismatch of the PET images and the CT based attenuation correction map, introducing artifacts in the PET image [7]. Due to the relatively high radiation dose associated with CT scans, it is undesirable to repeat the scan if motion occurs, particularly in children [8].

Several approaches to reducing motion artifacts in CT scans have been investigated. Li and colleagues investigated increasing rotation speed of the gantry to minimize motion effects [9]. This technique is restricted by the scanner's mechanical limits, and has the disadvantage of reducing the image signal-to-noise (SNR) ratio. Multi-acquisition or overlapping half-scan methods were also carried out by discarding motion corrupted image datasets and reconstructing an image from the remaining non-motion corrupted projections [10]. This method is not effective for constant motion, and increases patient dose. For respiratory or cardiac motion, gating methods are often used, however this requires a *priori* information about the cardiac or respiratory cycle with an assumption that the patient motion is periodic [11].

Some studies have suggested post-processing methods, which utilize known patient motion data to compensate for motion. Zerfowski [12] and Lu [13] used a mathematical approach to detect inconsistencies in the raw projection data and apply corrections in sinogram space. These methods are generally applicable to shifts but not rotations. They are limited to simple beam geometry and/or to a simple motion model. Westermann *et al.* measured patient motion during helical CT scans using an optical digitizer, and used this information to perform slice-by-slice image registration [14]. This method can correct for misalignments of reconstructed slices, but cannot remove motion effects such as distortion or blurring.

Manuscript received November 4, 2011. This work was supported by the Australian NHMRC Grants No. 571378 and 632677.

Jung-Ha Kim is with the Discipline of Medical Radiation Sciences, University of Sydney, NSW 2141, Australia (e-mail: jung.kim@sydney.edu.au).

Johan Nuyts is with the Department of Nuclear Medicine, Katholieke Universiteit, Leuven, Belgium (e-mail: johan.nuyts@uzleuven.be).

Zdenka Kuncic is with the School of Physics, University of Sydney, NSW 2050, Australia (e-mail: zdenka.kuncic@ sydney.edu.au).

Roger Fulton is with the School of Physics, University of Sydney, NSW 2050, Australia, and and Discipline of Medical Radiation Sciences, University of Sydney, NSW 2141, Australia as well as with the Department of Medical Physics, Westmead Hospital, NSW 2145, Australia. (e-mail: r.fulton@ physics.usyd.edu.au).

We have recently demonstrated in simulations the feasibility of correcting for rigid motion in spiral CT using knowledge of the motion during the scan, and fully 3D iterative reconstruction [15]. The aim of the present work was to devise a practical motion tracking method to record head motion during CT scanning, so that motion correction could be tested in actual CT scans. We have developed a method to calibrate an optical motion tracking system to a CT scanner coordinate system so that motion tracker data can be converted to CT scanner coordinates for use in motion correction. This process is more difficult than in PET [2] because the couch moves axially during the CT scan, and the portion of CT field of view that is actually imaged (both axially and in-plane) varies depending on the topogram that is selected prior to each scan. We here describe the calibration method, and its validation using a phantom to which known motion was applied.

II. Methods

A. CT Scanner and Motion Tracker Calibration

An optical motion tracking system (Polaris Hybrid Spectra, Northern Digital, Waterloo, Ontario, Canada) was used for motion tracking. This system can calculate the location of passive retro-reflective markers by detecting reflected infrared light (λ = 880 nm). Previous studies have used this system to measure motion for PET motion correction [2, 3]. For targets with 3 or more markers it can report the target pose as 3 rotations and 3 translations with root mean square positional error of 0.30mm within its measurement volume. A reference target comprising four retro-reflective disks 0.6 cm in radius was firmly attached to the gantry to enable use of differing measurement positions of the tracking system relative to the scanner. Since pose was reported in tracker coordinates, and motion correction requires motion in CT scanner coordinates, a calibration was performed to determine the transformation required to convert between the coordinate systems. The calibration method was similar to that used for PET and SPECT scanners in previous studies [2].

This calibration was carried out using a single retro-reflective disk marker (0.6 cm radius) on a plastic substrate that was placed on the bed of a Siemens Biograph 16 PET/CT scanner. The disk marker was centred over a hole in the substrate which made the marker centre identifiable in CT images. All experiments were performed using a standard pediatric head imaging protocol. Scan parameters were 120 kVp, 155 mA, pitch of 0.5 and a slice thickness of 1 mm while pose measurements were acquired at 20Hz with the motion tracker. After reconstruction the 3D location of the centre of the marker within the CT imaging volume was carefully identified.

Prior to performing a spiral CT scan, a planar topogram is acquired and the user interactively selects the bounds of the volume to be imaged. This sets certain parameters such as the origin of the image, image dimensions and pixel size, all of which are stored in the DICOM meta-data. The centre of the selected imaging volume can be several centimeters away from the isocenter. Therefore, there are 3 different coordinate systems involved in the calibration procedure. The definition of each coordinate system used is as follows:

- Tracker coordinate system: the inherent coordinate system of the optical tracker.
- Reference scanner coordinate system: the CT scanner coordinate system with origin on the rotation axis at the beam centre (isocenter of the scanner).
- Local imaging coordinate system: The coordinate system of the imaged volume defined by the operator. Its spatial relationship to the reference coordinate system is variable.

The voxel indices of the centre of the marker in the CT image were converted to the reference scanner coordinate system using the following equation:

$$\begin{bmatrix} P_x \\ P_y \\ P_z \\ 1 \end{bmatrix} = \begin{bmatrix} R_{00} & R_{10} & R_{20} & S_x \\ R_{01} & R_{11} & R_{21} & S_y \\ R_{02} & R_{12} & R_{22} & S_z \\ 0 & 0 & 0 & 1 \end{bmatrix} \begin{bmatrix} i\Delta i \\ j\Delta j \\ k\Delta k \\ 1 \end{bmatrix} \quad (1)$$

where P is the (x,y,z) position in reference scanner coordinates of the voxel (i,j,k) in the reconstructed image; R is the orientation matrix; S_x, S_y and S_z are the isocentre offsets of the top left voxel of slice 1 in x, y and z; and Δi, Δj, Δk are the x, y and z pixel sizes, respectively. Note that values of $S_{x,y,z}$ and Δi, Δj, Δk vary depending on the FOV defined on the topogram prior to the actual CT scan. S_x, Δi, Δj, *and* Δk These can be extracted from DICOM metadata i.e., however, S_y and S_z need to be calculated from information provided in the DICOM header as follows:

$$S_y = yoffset + bed\_height$$
$$S_z = -\left(\frac{total\_scan\_length}{2}\right) \quad (2)$$

where *yoffset* is defined as the minus distance in mm between the upper surface of the bed to the top left corner voxel of the image for the selected image volume, and *bed_height* is the distance from the isocenter of the scanner to the upper surface of the bed. Therefore, the summation of the *yoffset* and *bed_height* gives us the y coordinate of the top left corner voxel of the image in isocenter coordinate system as shown in Fig. 1. *total_scan_length* can be calculated from slice thickness and the number of slices in the CT image.

Position measurements of the sphere marker recorded by the Polaris Spectra optical tracker were taken at the mid-scanning point where z = 0 is at the centre of the total scan length. This was repeated for ? different positions of the marker at a variety of bed heights, imaging volumes. The transformation matrix, T_c, representing the relative rotation and displacement of the tracker and isocentre coordinate systems was then calculated by a closed form least squares method [2, 16].

Components	Uncertainty (mm)		
	x	*y*	*z*
Inherent uncertainty in tracker position measurement	0.30	0.30	0.30
CT image pixel sizes	0.30	0.30	0.50
Uncertainty in position at mid scan point	0.1	0.2	0.3
Total uncertainty (mm)	0.4	0.5	0.7

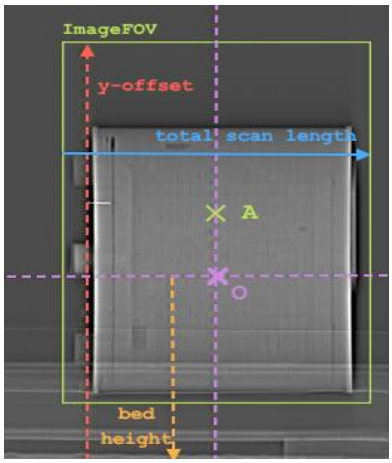

Fig. 1. Schematic diagram of a topogram for Hoffman brain phantom. Point A and O corresponds to center of the local image coordinates and isocenter of the reference CT scanner coordinates, respectively.

An analysis of the measurement uncertainties contributing to the calibration was then performed, taking into account the inherent variability in Polaris position measurements as quoted by the manufacturer, a half of the CT image pixel size, and the measured s.d. of Polaris position measurements in the vicinity of the mid-scan point, which is dependent on the setup of the equipment. The total uncertainty was calculated in each axis as the square root of the sum of the squares of the above components.

B. Validating the Calibration

Two CT scans (scan1 and scan2) of a stationary Hoffman 3D brain phantom, with an attached retro-reflective target, were acquired with the phantom in different poses. Pose measurements were taken at the maximum sampling rate of the tracker (60 Hz) during each CT acquisition. The motion between scan1 and scan2 was calculated from the change in target pose as observed by the tracker, converted to CT coordinates using T_c, and applied to one of the reconstructed image volumes. The spatial match of the image volumes was then assessed by choosing landmarks on the slices (Fig. 2), and comparing the voxel indices of these landmarks in the row, column and slice directions. This procedure was repeated 14 times and the voxel indices averaged

As the tracker was repositioned between the calibration and the validation experiments, T_c was recalculated based on the change in apparent position of the reference target. Differences between the topograms used for calibration and the validation scans were also taken into account.

TABLE I. UNCERTAINTIES IN CALIBRATION PROCEDURE.

III. RESULTS AND DISCUSSION

The T_c derived from the calibration procedure fitted the calibration data well, with maximal deviations between predicted and measured marker positions of less than 0.8 mm in *x*, *y*, and *z*. Table I lists the components of the total uncertainty in these measurements.

Fig 2 shows a comparison of the two CT scans of the Hoffman brain phantom before and after movement. images Images superimposed in (A) and (C), that demonstrate clear displacement of the object. Fig 2 (B) and (D) images were obtained by applying the calculated motion to after movement images in (A) and (C), respectively. Measured landmark displacements are shown in Table II and were …. Mean registration errors between the predicted images and original images were estimated from landmark analysis by choosing 3 slices of the images that are well-spaced and at least 3 landmarks per each slice: 0.16 mm ± 0.4 mm, 0.24 mm ± 0.5 mm, and less than 0.17 mm ± 0.7 mm in *x*, *y*, and *z*, respectively.

Image profiles are shown in Fig 3. Although some large differences are evident in CT numbers, which is mainly due to interpolation of the pixel values, all edges are very well matched positionally in the original and moved scans.

These results indicate the feasibility of optical motion tracking in CT scans with sub-millimeter precision. We expect that current registration errors could be reduced by using a marker with a more easily identifiable centre, and using Polaris data obtained with the bed stationary rather than attempting to obtain a marker position measurement at the mid-point of the scan, which has the limitation that no pose measurement may correspond exactly to the desired position.

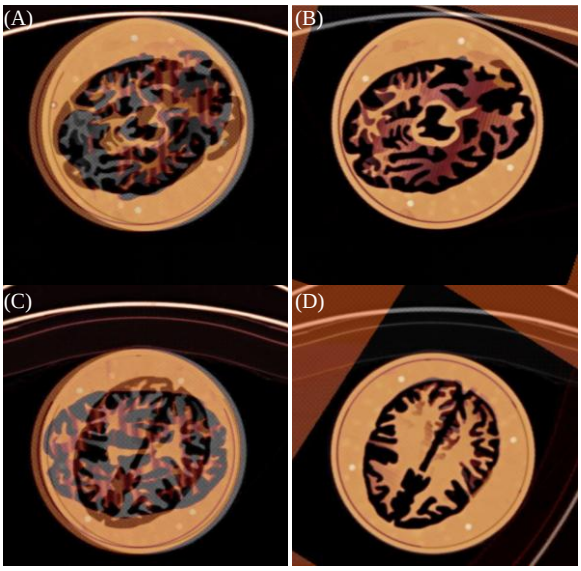

Fig. 2. Two CT images overlaid with corresponding slice number: (A) and (C) Two original images of before- (gray) and after-movement (red) with ycenter value of 0 and -30, respectively; (B) and (D) Before-movement image (grey) with corrected after-movement images (red) with ycenter value of 0 and -30, respectively.

TABLE II. LANDMARK DISPLACEMENTS BETWEEN SCAN1 AND (MOVED) SCAN2

Axis	Differences		
	Mean (mm)	Max (mm)	s.d.
x	0.16	1.17	0.66
y	0.24	1.76	0.72
z	0.17	1.0	0.17

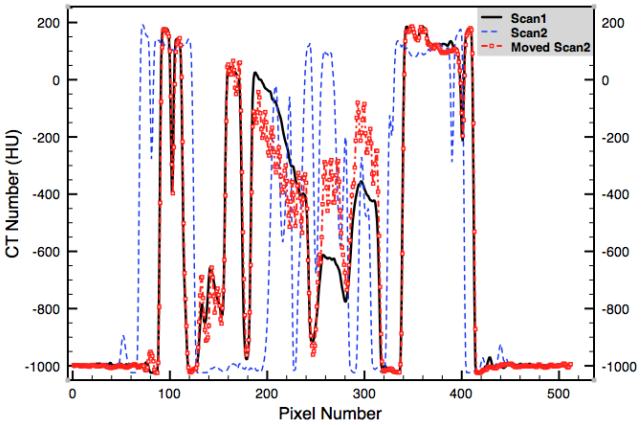

Fig. 3. A comparison of CT numbers along the *x*-axis of scan1, scan2 and calculated motion applied scan2 at the same slice and a pixel number in *y*-axis.

Some of our studies, where a large rotation motion was applied, show poorer agreement between the original and moved CT scans than others, which requires a further investigation. However, the error increase is only noticeable when the rotation is larger than about 130°, which is unlikely to occur in patients.

IV. CONCLUSION

We have successfully implemented an optical motion tracking method for CT scanning and validated the derived motion measurements in CT coordinates in a series of paired phantom experiments. In these experiments the two CT scans were registered by applying a spatial transformation derived from motion tracker data converted to CT coordinates using a separately derived calibration transformation. Positional errors were at worst 1.8 mm of the correct value in the *y* direction, and averaged < 0.25 mm in all directions. While a lesser degree of error would be desirable for motion correction, this degree of accuracy should be sufficient to enable substantial reduction of motion artifacts. We will pursue improved accuracy in future work by further refinements to our technique. Our next goal is to trial our motion tracking method in attempts to compensate for the rigid motion of an object during actual spiral CT scans. There are still some challenges in motion correcting CT scans such as the accurate synchronisation of tracker and scanner data, and the limited sampling rate of the motion tracking system.

ACKNOWLEDGMENT

This work was supported by NHMRC Grants 571378 and 632677.

REFERENCES

[1] S. C. Kaste, "Issues specific to implementing PET-CT for pediatric oncology: what we have learned along the way," *Pediatr. Radiol.*, vol. 34, pp. 205-213, 2004.

[2] R. R. Fulton, *et al.*, "Correction for head movements in positron emission tomography using an optical motion tracking system," *IEEE Trans. Nucl. Sci.*, vol. 49, pp. 116-123, 2002.

[3] P. M. Bloomfield, *et al.*, "The design and implementation of a motion correction scheme fore neurological PET," *Phys. Med. Biol.*, vol. 48, pp. 959-978, 2003.

[4] R. Popilock, *et al.*, "CT Artifact Recognition for the Nuclear Technologist," *J Nucl Med Technol*, vol. 36, pp. 79-81, 2008.

[5] A. Wagner, *et al.*, "Quantification and Clinical Relevance of Head Motion During Computed Tomography," *Investigative Radiology*, vol. 38, pp. 733-741, 2003.

[6] A. Plessis, *et al.*, "The effects of misinterpretation of an artefact on multidetector row CT scans in children," *Pediatr Radiol*, vol. 39, pp. 137-141, 2009.

[7] C. Liu, *et al.*, "Respiratory motion correction for quantitative PET/CT using all detected events with internal-external motion correction," *Med. Phys*, vol. 38, pp. 2715-2723, 2011.

[8] D. J. Brenner, *et al.*, "Estimated Risks of Radiation-Induced Fatal Cancer from Pediatric CT," *American Journal of Roentgenology*, vol. 176, pp. 289-296, 2001.

[9] L. Li, *et al.*, "Experimental measurement of human head motion for high-resolution computed tomography system design," *Optical Engineering* vol. 49, 2010.

[10] D. Parker, *et al.*, "Dose minimization in computed tomography overscanning," *Med. Phys.*, vol. 8, pp. 706-11, 1981.

[11] C. Schretter, *et al.*, "Image-based iterative compensation of motion artifacts in computed tomography," *Med. Phys.*, vol. 36, pp. 5323-5330, 2009.

[12] D. Zerfowski, "Motion Artifact Compensation in CT," Institut für Algorithmen und Kognitive Systeme., Universität Karlsruhe, 1998.

[13] W. Lu and T. Mackie, "Tomographic motion detection and correction directly in sinogram space," *Phys. Med. Biol.*, vol. 47, pp. 1267-1284, 2002.

[14] B. Westermann and R. Hauser, "Online Head Motion Tracking Applied to the Patient Registration Problem," *Computer Aided Surgery*, vol. 5, pp. 137-147, 2000.

[15] J. Nuyts, presented at the Fully 3D meeting, 2011.

[16] B. K. P. Horn, "Closed-form solution of absolute orientation using unit quaternions," *J. Optical Soc. Amer.*, vol. 4, pp. 629-642, 1987.